CASE REPORT

Tumor-Induced Osteomalacia in a Patient With *FGF23*-Amplified Lung Adenocarcinoma and *FGF23*-Deleted SCLC: Case Report

Marcello Moro Queiroz, MD,[a,*] Ricardo Dahmer Tiecher, MD,[a] João Felipe Lima Feldmann, MD,[a] Elisangela Monteiro Coser, BSc,[b] Mariana Vargas Cruz, PhD,[c] Livia Loureiro, PhD,[d] Gabriela Franco Katz, MD,[e] Marina Henkin Behar, MD,[a] João Victor Machado Alessi, MD,[a] Leonardo de Abreu Testagrossa, PhD,[c] Anamaria Aranha Camargo, PhD,[b] Paula Fontes Asprino, PhD,[b] Fabiana Bettoni, PhD,[b] Artur Katz, MD[a]

[a]*Oncology Center, Hospital Sírio-Libanês, São Paulo, São Paulo, Brazil*
[b]*Molecular Oncology Center, Hospital Sírio-Libanês, São Paulo, São Paulo, Brazil*
[c]*Department of Pathology, Hospital Sírio-Libanês, São Paulo, São Paulo, Brazil*
[d]*Medical Affairs Organization, Illumina, São Paulo, São Paulo, Brazil*
[e]*University of Central Lancashire, Preston, United Kingdom*

Received 25 November 2024; revised 19 February 2025; accepted 5 March 2025
Available online - 8 March 2025

ABSTRACT

Tumor-induced osteomalacia (TIO) is a rare paraneoplastic syndrome characterized by ectopic fibroblast growth factor-23 (FGF23) production. We report a unique case of a 78-year-old female patient with refractory hypophosphatemia, ultimately diagnosed as TIO, in the context of two metastatic primary lung cancers: adenocarcinoma and SCLC. Molecular analyses of tumor samples highlighted *FGF23* amplification in one adenocarcinoma sample and *FGF23* deletion in one SCLC sample, suggesting a potential link between tumor *FGF23* molecular alterations and elevated serum FGF23 levels. This case underscores the complexity of diagnoses and management of TIO when associated with solid tumors and highlights the need for awareness of this condition to prevent diagnostic delays. Future research should explore the mechanisms linking *FGF23* alterations and cancer progression and evaluate targeted therapies for TIO in the context of resistant metastatic cancers.

Keywords: Tumor-induced osteomalacia; Lung adenocarcinoma; Fibroblast growth factor-23; Case report

Introduction

Tumor-induced osteomalacia (TIO) is a rare paraneoplastic syndrome caused by tumor cells' ectopic production of fibroblast growth factor-23 (FGF23).[1] A recent literature review suggests approximately 2000 TIO cases have been reported.[2]

FGF23 is a phosphaturic hormone produced by osteoblasts and osteocytes. It inhibits phosphate reabsorption in the kidneys and reduces 1,25-dihydroxyvitamin D production, lowering gastrointestinal phosphorous absorption. Excessive FGF23 leads to hypophosphatemia, low or inappropriately normal 1,25-dihydroxyvitamin D, and clinical osteomalacia.[3,4]

***Corresponding author.**

Address for correspondence: Marcello Moro Queiroz, MD, Oncology Center, Hospital Sírio-Libanês, Street Adma Jafet, number 115, São Paulo, São Paulo, 01308-050, Brazil. E-mail: marcello.mqueiroz@hsl.org.br

Cite this article as: Queiroz MM, Tiecher RD, Feldmann JFL, et al. Tumor-induced osteomalacia in a patient with *FGF23*-amplified lung adenocarcinoma and *FGF23*-Deleted SCLC: case report. *JTO Clin Res Rep*. 2025;6:100822.

ISSN: 2666-3643

https://doi.org/10.1016/j.jtocrr.2025.100822

TIO most often arises from ectopic FGF23 production by phosphaturic mesenchymal tumors owing to a fibronectin 1 (FN1)–FGFR1 fusion.[5] The role of other tumors, such as lung cancers, in inducing TIO is less well understood, with their underlying molecular mechanisms remaining largely unexplored.

We report a case of TIO in a patient with two concomitant metastatic lung cancers: adenocarcinoma and SCLC. We highlight the molecular characteristics of both tumors, confirming they were both primary, and explore the potential association between lung adenocarcinoma and the subsequent TIO.

Case Report

A 78-year-old female patient, an active smoker (70 pack-y) with a history of chronic obstructive pulmonary disease, presented with a new right lung nodule (1.4 × 0.7 × 1.2 cm) on computed tomography (CT). Enlarged mediastinal and supraclavicular lymph nodes were also noted.

The patient was diagnosed with stage IIIC (American Joint Committee on Cancer, eighth edition) adenocarcinoma of the right lung. Lymph node involvement was confirmed through a core biopsy of the right supraclavicular lymph node (sample 1) and endobronchial ultrasound–guided fine-needle aspiration of the mediastinal lymph nodes. Programmed death-ligand 1 expression was 90% (Ventana programmed death-ligand 1 SP263 Assay), and a commercial next-generation sequencing eight–cancer gene panel analysis (*AKT1*, *BRAF*, *EGFR*, *ERBB2*, *KRAS*, *NRAS*, *MET*, and *PIK3CA*) detected a *KRAS* G12C mutation. The patient underwent concomitant chemoradiation therapy, followed by 14 months of consolidation therapy with durvalumab.

Nineteen months after consolidation therapy, the adenocarcinoma recurred in the central nervous system (CNS) as a single lesion, which was surgically resected (sample 2). Although surgical bed radiation was employed, systemic treatment was not initiated because imaging found no other systemic lesions.

Eighteen months later, the patient was diagnosed with limited-stage SCLC. An 18F-labeled fluorodeoxyglucose positron emission tomography–CT scan revealed increased uptake in a new right perihilar nodule, ipsilateral hilar lymph node, and a contralateral mediastinal lymph node, which was confirmed by endobronchial ultrasound–guided fine-needle aspiration of the lymph nodes (sample 3). At this time, the patient's phosphate level was slightly decreased (2.3 mg/dL). No previous measurements were available to determine the onset of hypophosphatemia accurately.

The patient was treated with concurrent chemoradiation with curative intent. Nevertheless, four months after completing treatment, a positron emission tomography–CT scan revealed disease relapse, with new lesions in the bones, liver, and lymph nodes. A biopsy of the left supraclavicular lymph node (sample 4) confirmed metastatic SCLC. Considering a platinum-resistant SCLC relapse and a strong preference of the patient for oral treatment, the patient began receiving olaparib and temozolomide.[6]

After reporting muscle weakness and fatigue, the patient was found to have severe hypophosphatemia (0.8 mg/dL). Serum FGF23 was elevated at 509 relative unit/mL, and TIO was diagnosed. Table 1 summarizes the patient's laboratory test results during TIO diagnosis, and Figure 1 illustrates the key diagnostic and treatment milestones.

We performed a detailed genomic analysis of archival tumor samples using a comprehensive tumor panel sequencing TSO500 (Illumina Inc.). Four samples were sequenced, as shown in Table 2. The complete methodology of the analysis is provided in the Supplementary Material.

Sequencing of the patient's adenocarcinoma samples revealed a *KRAS* G12C mutation in both. In addition, the CNS metastasis reported *FGF23* amplification and *FGF6* amplification. In contrast, the SCLC samples exhibited inactivating mutations in *TP53* and *RB1*, characteristics of this disease.[7] These SCLC samples also shared heterozygous deletions, including *KRAS*, *FGF23,* and *CCND3*. A complete list of somatic genomic alterations is detailed in Table 2.

Discussion

This case report presents an exceptionally rare paraneoplastic syndrome associated with malignant solid tumors: TIO. Although it has been previously reported in patients diagnosed with SCLC,[2,8] we discuss a unique case involving a patient with two primary lung cancers: adenocarcinoma and SCLC. In addition, we explore a potential link between the emergence of TIO and the molecular alterations found in the patient's lung adenocarcinoma, a histologic subtype not often associated with this paraneoplastic syndrome. To our knowledge, this is the first reported case of lung adenocarcinoma associated with TIO in which the potential molecular basis has been described.

Molecular analysis revealed distinct profiles between the adenocarcinoma and SCLC samples, with no shared mutations (Table 2). The considerable genetic differences between the tumors, with no common somatic mutations identified, support the hypothesis of two independent primary tumors and reduce the likelihood of phenotypic transformation. It also revealed shared somatic alterations between the primary lung adenocarcinoma and the

Table 1. Patient's Laboratory Tests at the Time of Diagnosis of Tumor-Induced Osteomalacia

Laboratory Test	Value	Reference Range
FGF23, plasma (RU/mL)	509	up to 180
Phosphorus (mg/dL)	0.8	2.5-4.5
PTH (pg/mL)	31	10-65
PTHrp (pg/mL)	10	11-20
Calcitriol (pg/mL)	16	18-72
25-hydroxyvitamin D3 (ng/mL)	37	>20
25-hydroxyvitamin D2 (ng/mL)	<5	<5

FGF23, fibroblast growth factor-23; PTH, parathyroid hormone; PTHrp, PTH-related protein; RU, relative unit.

CNS metastasis, confirming their common origin. Nevertheless, the metastasis may have acquired additional gene amplifications as it exhibited further alterations, including *FGF23* amplification, potentially leading to the onset of TIO. Alternatively, limitations in the sample analysis, including low cellularity in sample 1 (20%), could have affected the detection of gene amplifications, explaining why *FGF23* amplification was only identified in sample 2. In addition, sample 2 was negative for TTF-1, despite sample 1 being TTF-1–positive. Both analyses were conducted using the same antibody (Ventana 8G7G3/1). This discrepancy may be explained by clonal selection after the treatment of the adenocarcinoma with chemoradiotherapy and immunotherapy. Histologic images of both samples, which are included in the Supplementary Material (Supplementary Fig. 1), reveal that the samples exhibited similar morphologic characteristics.

FGF23 amplification is rare in cancer. In the International Cancer Genome Consortium and The Cancer Genome Atlas pan-cancer data set, *FGF23* amplification is observed in 5.1% of patients across various cancer types. Among these, only 5.3% of cases involved non-SCLC, all of which were squamous cell carcinomas.[9] *FGF23* amplification has been reported in only a few TIO cases associated with malignant tumors. For instance, one case of SCLC exhibited both FGF23 immunostaining and *FGF23* amplification.[8] The overall prevalence of *FGF23*

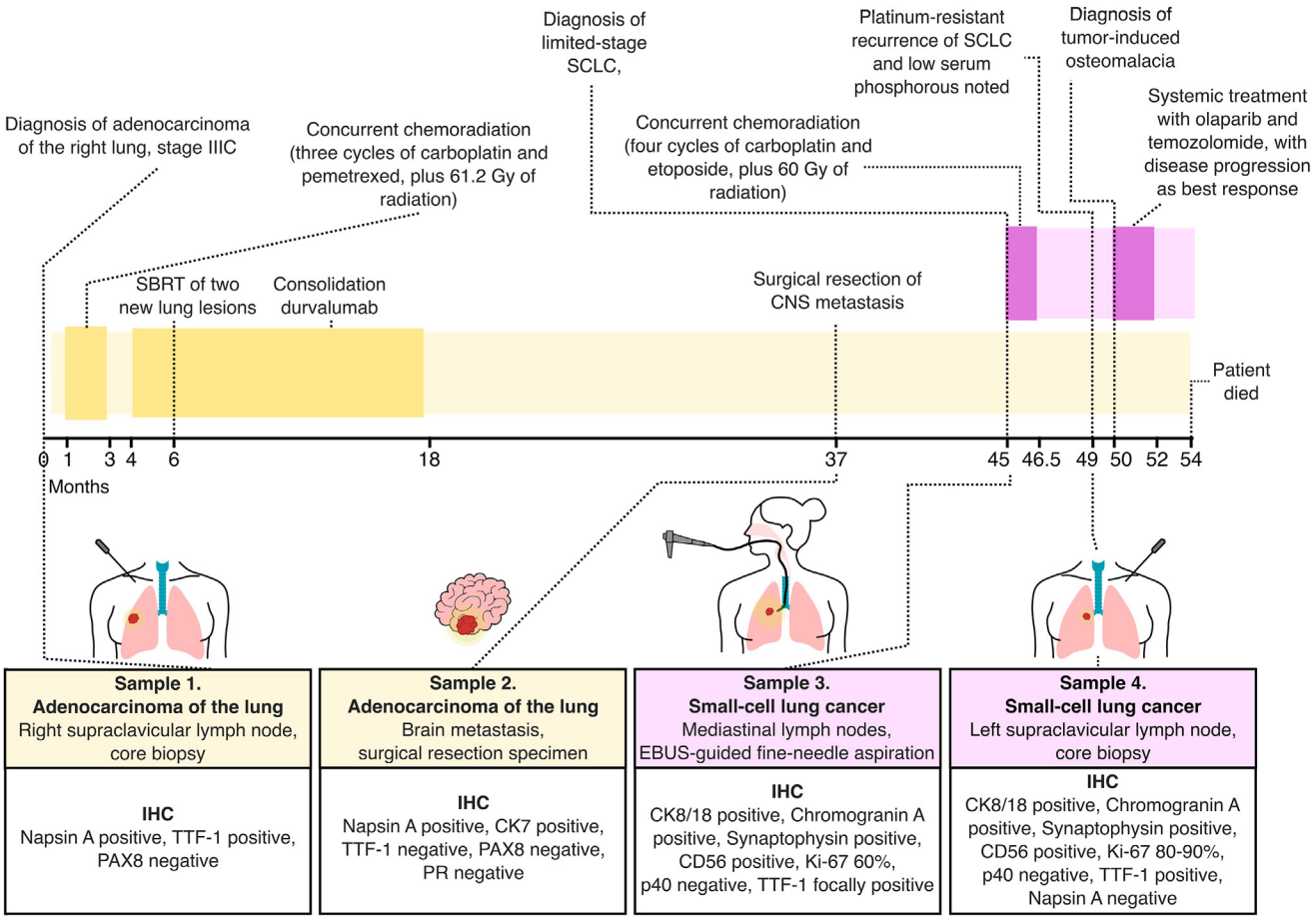

Figure 1. Timeline highlighting key diagnostic and treatment milestones, from initial diagnosis to end-of-life care. This figure was created using Inkscape (inkscape.org). CD, cluster of differentiation; CK, cytokeratin; CNS, central nervous system; EBUS, endobronchial ultrasound; Gy, gray; IHC, immunohistochemistry; Ki, Antigen Kiel; PAX, paired-box; PR, progesterone receptor; SBRT, stereotactic body radiotherapy; TTF, thyroid transcription factor.

Table 2. Molecular Analysis of Four Tumor Samples Performed With the NGS Cancer Panel

Biomarker	Sample 1	Sample 2	Sample 3	Sample 4
Microsatellite status	Stable	Stable	Stable	Stable
TMB	1.6 muts/Mb	24.3 muts/Mb	10.9 muts/Mb	9.4 muts/Mb
Gene fusions	NA	NA	NA	Not detected
Splice variants	NA	NA	NA	*MET* aberrant isoform (rearrangement within exon 2)
Gene amplifications	Not detected	*FGF23*: 10.9 copies *FGF6*: 11.2 copies *KRAS*: 10.3 copies *MDM2*: 3.3 copies *ALK*: 3.0 copies	*PIK3CA*: 3.3 copies	*PIK3CA*: 3.3 copies *MYCL*: 3.2 copies
Gene deletions (heterozygous)	Not detected	*LAMP1*	*RAF1* *CCND3* *FGF23* *KRAS*	*RAF1* *CCND3* *FGF23* *KRAS* *FGF6* *BRCA2*
Tumor cellularity estimation	20%	100%	90%	100%
Small variants (SNVs or indels) (Gene, Protein change, VAF)	*KRAS* G12C (6%) *NRG1* S633* (2%) *CDKN2A* T77Pfs*40 (2%) *AR* D266N (2%) *AR* G106C (3%) *BCOR* G1463V (2%) *ANKRD11* K1461Rfs*93 (1.2%)	*KRAS* G12C (82%) *NRG1* S633* (61%) *CDKN2A* T77Pfs*40 (67%) *AR* D266N (41%) *AR* G106C (41%) *BCOR* G1463V (42%) *BCOR* A320V (46%) *ADGRA2* N336K (56%) *AR* L345V (39%) *ARID1A* E1735Q (71%) *ARID1A* E1776* (63%) *AXIN1* S75N (24%) *BRIP1* D602H (29%) *CASP8* M169I (29%) *EPHA3* D130Y (24.2%) *GEN1* H260N (1.6%) *IRS1* D241Y (34%) *MCL1* P122S (24%) *MED12* F102L (17%) *MED12* S1602W (13%) *PAK5* M652I (29%) *PPP2R1A* D515A (3%) *RBM10* P597T (47%) *RBM10* V16F (20%) *SMC1A* E679* (35%) *TBX3* S574F (23.5%) *TRAF2* E126* (61%)	*RB1* K640* (70%) *TP53* V272L (74%) *BMPR1A* K60M (26%) *BRAF* I61V (44%) *ERCC5* D79Y (41%) *GREM1* F117L (41%) *KAT6A* E750A (42%) *PTPRT* Q1418K (45%) *SMAD3* R142H (21%) *STAG2* C527Y (33%) *TET2* T1726A (43%) *CTNNB1* M731I (1.7%) *DIS3* V502F (3.3%) *FGF4* S54L (9%) *MAP3K4* N160Mfs*8 (1.7%) *WT1* P179L (12%)	*RB1* K640* (78%) *TP53* V272L (82%) *BMPR1A* K60M (45%) *BRAF* I61V (45%) *ERCC5* D79Y (41%) *GREM1* F117L (45%) *KAT6A* E750A (42%) *PTPRT* Q1418K (45%) *SMAD3* R142H (39%) *STAG2* C527Y (42%) *TET2* T1726A (45%) *CARD11* A701S (1.4%) *CUX1* R254K (1%) *PBRM1* A362G (5.3%)

Only confirmed somatic tumor-specific mutations are presented.
Sample 1: right supraclavicular lymph node; sample 2: brain metastasis; sample 3: right lower paratracheal lung lesion and left lower paratracheal lymph node; sample 4: left supraclavicular lymph node.
Only sample 4 had the RNA evaluated for gene fusions and splice variants.
MSI, microsatellite instability; muts/Mb, mutations per megabase; NA, not analyzed; NGS, next-generation sequencing; SNV, single nucleotide variant; TMB, tumor mutational burden; VAF, variant allele frequency.

amplification leading to TIO is unknown, even in tumors that harbor this alteration.

Although there was no histologic confirmation of adenocarcinoma recurrence after the CNS metastasis, the disease had already been identified as metastatic when the patient developed TIO. The biopsy confirming SCLC progression was performed on a lymph node, the most accessible site for biopsy. Nevertheless, in retrospect, we cannot exclude the possibility that one of the other sites of disease progression, such as bones and liver, might have contained remnants of the previously active metastatic adenocarcinoma. Given the *FGF23* amplification in the adenocarcinoma cells and the loss of heterozygosity of *FGF23* in the SCLC tumors, it is plausible that viable adenocarcinoma cells likely persisted and were responsible for the elevated plasma FGF23 levels and TIO.

In cases of TIO, a reduction of plasma FGF23 levels and improvement in serum phosphate levels have been reported after successful systemic anticancer treatment.[10] Nevertheless, in this case, the patient experienced a rapid decline in performance and did not respond to anticancer therapy after the SCLC recurrence. At that time, the possibility that TIO might be associated with residual adenocarcinoma cells was not considered, as molecular analysis was only available postmortem, and additional tests, such as liquid biopsies, could not be performed. Despite ongoing supportive care with recurrent electrolyte corrections, the patient ultimately succumbed.

In conclusion, this case contributes to the limited but expanding knowledge of solid tumors associated with TIO and, to our knowledge, represents the first case report where comprehensive molecular analyses suggested a molecular basis for ectopic FGF23 production in a patient with lung adenocarcinoma. Although an *FGF23* deletion was observed in the SCLC sample, the possibility of TIO secondary to SCLC cannot be excluded, given the temporal correlation between the two conditions. Taken together, these findings suggest that molecular alterations in the *FGF23* pathway may contribute to TIO development regardless of tumor subtype. Future studies should investigate the mechanistic links between *FGF23* amplification/deletion and cancer progression and explore optimized treatment strategies for managing TIO in the setting of treatment-resistant, metastatic cancers.

CRediT Authorship Contribution Statement

Marcello Moro Queiroz: Conceptualization, Methodology, Writing - original draft, Writing - review & editing, Final approval, Supervision.

Ricardo Dahmer Tiecher: Conceptualization, Methodology, Writing - original draft, Writing - review & editing, Final approval, Supervision.

João Felipe Lima Feldmann: Conceptualization, Writing - original draft, Writing - review & editing, Final approval, Supervision.

Elisangela Monteiro Coser: Methodology, Writing - review & editing, Final approval.

Mariana Vargas Cruz: Methodology, Writing - review & editing, Final approval.

Livia Loureiro: Resources, Writing - review & editing, Final approval, Funding acquisition.

Gabriela Franco Katz: Writing - original draft, Writing - review & editing, Final approval.

Marina Henkin Behar: Writing - original draft, Writing - review & editing, Final approval.

João Victor Machado Alessi: Writing - original draft, Writing - review & editing, Final approval.

Leonardo de Abreu Testagrossa: Resources, Writing - review & editing, Final approval.

Anamaria Aranha Camargo: Resources, Writing - review & editing, Final approval, Funding acquisition.

Paula Fontes Asprino: Conceptualization, Methodology, Writing - original draft, Writing - review & editing, Final approval, Supervision.

Fabiana Bettoni: Conceptualization, Methodology, Writing - original draft, Writing - review & editing, Final approval, Supervision.

Artur Katz: Conceptualization, Writing - review & editing, Final approval, Supervision.

Disclosure

The authors declare no conflict of interest.

Acknowledgments

The authors would like to acknowledge the patient described in this report for allowing us to provide her care and for granting written consent for the publication of this work. This work was supported by Hospital Sírio-Libanês and the Medical Affairs Organization, Illumina, San Diego. Both institutions provided all the reagents for the molecular analyses described in this study.

Informed Consent Statement

Written informed consent was obtained from the patient for the publication of this case report.

Declaration of Generative AI and AI-Assisted Technologies in the Writing Process

During the preparation of this work the authors used ChatGPT 4.0 to improve readability. After using this tool, the authors reviewed and edited the content as needed and take full responsibility for the content of the publication.

Supplementary Data

Note: To access the supplementary material accompanying this article, visit the online version of the *JTO Clinical and Research Reports* at www.jtocrr.org and at https://doi.org/10.1016/j.jtocrr.2025.100822.

References

1. Jonsson KB, Zahradnik R, Larsson T, et al. Fibroblast growth factor 23 in oncogenic osteomalacia and X-linked hypophosphatemia. *N Engl J Med*. 2003;348:1656–1663.
2. Rendina D, Abate V, Cacace G, et al. Tumor-induced osteomalacia: a systematic review and individual Patient's data analysis. *J Clin Endocrinol Metab*. 2022;107:e3428–e3436.
3. Urakawa I, Yamazaki Y, Shimada T, et al. Klotho converts canonical FGF receptor into a specific receptor for FGF23. *Nature*. 2006;444:770–774.
4. Bosman A, Palermo A, Vanderhulst J, et al. Tumor-induced osteomalacia: a systematic clinical review of 895 cases. *Calcif Tissue Int*. 2022;111:367–379.
5. Liu X, Yin X, Li D, et al. RNA sequencing reveals novel oncogenic fusions and depicts detailed fusion transcripts of FN1-FGFR1 in phosphaturic mesenchymal tumors. *Mod Pathol*. 2023;36:100266.
6. Farago AF, Yeap BY, Stanzione M, et al. Combination olaparib and temozolomide in relapsed small-cell lung cancer. *Cancer Discov*. 2019;9:1372–1387.
7. George J, Lim JS, Jang SJ, et al. Comprehensive genomic profiles of small cell lung cancer. *Nature*. 2015;524:47–53.
8. Sauder A, Wiernek S, Dai X, et al. FGF23-associated tumor-induced osteomalacia in a patient with small cell carcinoma: a case report and regulatory mechanism study. *Int J Surg Pathol*. 2016;24:116–120.
9. ICGC/TCGA Pan-Cancer Analysis of Whole Genomes Consortium. Pan-cancer analysis of whole genomes. *Nature*. 2020;578:82–93.
10. AlHamer B, Singh A, Patrascu C, Al Mukaddam M. Tumor-induced osteomalacia due to sarcomatoid non–small cell lung carcinoma confounded by drug-induced Fanconi syndrome. *JCEM Case Rep*. 2024;2:luae101.